RAPID COMMUNICATIONS

PHYSICAL REVIEW A VOLUME 52, NUMBER 1 JULY 1995

Theory of longitudinal recoil-ion momentum distribution in ion-atom ionization

V.D. Rodríguez,* Y.D. Wang, and C.D. Lin

J.R. Macdonald Laboratory, Department of Physics, Kansas State University, Manhattan, Kansas 66506

(Received 24 March 1995)

The longitudinal recoil-ion momentum distributions of single ionization in collisions between fast heavy ions and atoms are analyzed by exploring the three-body kinematics and its relation to dynamic processes. It is found that there is a kinematic threshold for the longitudinal recoil-ion momentum distributions that can be ascribed to electron capture to the continuum (ECC). The finite cross section at threshold provides unambiguous evidence of the divergence of the ECC peak when the electron velocity is equal to the projectile velocity. Other aspects associated with the ionization process, such as soft-electron emission and binary-encounter collision, are also studied. Theoretical longitudinal recoil-ion momentum distributions are also compared to existing experiments.

PACS number(s): 34.10.+x, 34.50.Fa

The development of the recoil-ion momentum spectroscopy technique has provided new opportunities for studying ion-atom collisions physics in detail [1,2]. Until quite recently, much of our understanding of ionization dynamics in ion-atom collisions has come from the study of single and double differential cross sections of the projectile and/or of the emitted electron. In fact, the recoil ion carries as much information on the three-body ionization dynamics as the projectile and the electron. In this paper, we provide a theoretical analysis of the longitudinal recoil-ion momentum distribution in ionizing collisions between fast bare ions and atomic targets. Fundamental features characterizing ionization processes, such as electron capture to the continuum, soft-electron emission, and binary encounter collision, are studied by considering the longitudinal recoil-ion momentum distribution.

Dynamic constraints required by energy and momentum conservation are fundamental to the study of three-body ionization. In the laboratory frame, the longitudinal momentum conservation equation gives

$$p_{R||}=p_{P||}-p_{e||}=(\varepsilon_e-\varepsilon_i)/v-k_e\cos\theta_e\,, \tag{1}$$

where $p_{R||}$ and $p_{e||}$ are, respectively, the longitudinal momenta for the recoil ion and the ionized electron, and $p_{P||}$ is the longitudinal projectile momentum transfer. The momentum (energy) of the ionized electron is given by $k_e(\varepsilon_e=\frac{1}{2}k_e^2)$. The electron emission angle is given by θ_e. ε_i is the binding energy of the initial target electron. Equation (1) is correct to $O(1/M_p)$ and $O(1/M_t)$, where M_p (M_t) is the mass of the heavy projectile (target). Information on the longitudinal momentum distributions for the three charged particles can be determined by this equation. For a given $p_{R||}$, the longitudinal recoil-ion momentum distribution can be obtained by integrating the DDCS over the electron energy [in this paper, we always use DDCS to denote the double differential ionization cross section in *electron* emission angle and energy, i.e., $d^2\sigma/d\varepsilon_e d(\cos\theta_e)$],

$$\frac{d\sigma}{dp_{R||}}=\int_{\varepsilon_e^-}^{\varepsilon_e^+}\frac{1}{k_e}\frac{d^2\sigma}{d\varepsilon_e d(\cos\theta_e)}\,d\varepsilon_e\,. \tag{2}$$

The integration limits can be obtained from Eq. (1) or

$$k_e^{\pm}(\theta_e)=v\,\cos\theta_e\pm\sqrt{v^2\cos^2\theta_e+2(p_{R||}v-|\varepsilon_i|)} \tag{3}$$

with $\varepsilon_e^{\pm}=\frac{1}{2}(k_e^{\pm})^2$. Much information about the longitudinal recoil-ion momentum distribution can be obtained directly from this basic equation of three-body kinematics. In Fig. 1, we illustrate the relation among the three variables k_e, $p_{R||}$, and θ_e. For illustration, we choose $v=\sqrt{10}$ a.u. and binding energy $\varepsilon_i=-0.903$ a.u., corresponding to the ionization of the He atom by heavy ions at 250 keV/u. We emphasize that the analysis and discussion below should be general and do not depend on these parameters.

Electron capture to the continuum (ECC). The first interesting result is the existence of a threshold in the longitudinal recoil-ion momentum given by

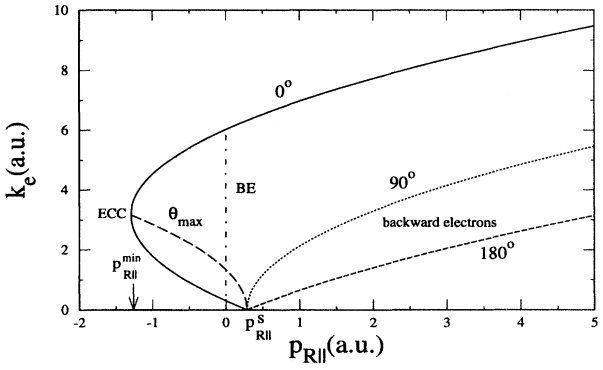

FIG. 1. Illustration of the kinematic relation between the longitudinal recoil-ion momentum and the ionized electron momentum at different electron emission angles. The symbols are explained in the text.

*Permanent address: Departamento de Física, Facultad de Ciencias Exactas y Naturales, Universidad de Buenos Aires, 1428 Buenos Aires, Argentina.

$$p_{R||}^{min}=-\frac{v}{2}+\frac{|\varepsilon_i|}{v}, \tag{4}$$

at which electrons are emitted at *zero degree* with the same velocity v as the projectile. In Fig. 1, at $\theta_e=0$, $p_{R||}=p_{R||}^{min}$, the two branches of the electron momentum function converge to a single value, $k_e^+=k_e^-=v$. This situation clearly corresponds to electron capture to the continuum, which gives rise to a cusp (divergence) in the observed DDCS spectra [3,4].

We next show that the longitudinal recoil-ion momentum distribution $d\sigma/dp_{R||}$ is *finite* at the threshold. For this purpose, we study the behavior of $d\sigma/dp_{R||}$ in the neighborhood of $p_{R||}^{min}$ $(\lambda\rightarrow 0)$,

$$p_{R||}=p_{R||}^{min}+2\lambda^2 v. \tag{5}$$

Near the ECC peak, we adopt the conventional parametrization for the DDCS [5]

$$\frac{d^2\sigma}{d\varepsilon_e d(\cos\theta_e)}=2\pi k_e|f_c(a_p)|^2\sum_{nl}B_{nl}(v)\left(\frac{p}{v}\right)^n P_l(\cos\theta'), \tag{6}$$

where $\vec{p}=\vec{k}_e-\vec{v}$ is the relative momentum of the electron with respect to the projectile, $\cos\theta'=\vec{v}\cdot\vec{p}/vp$, and f_c is the Coulomb factor

$$|f_c(a_p)|^2=\frac{2\pi a_p}{1-\exp(-2\pi a_p)}, \tag{7}$$

where $a_p=Z_p/p$, with Z_p being the projectile nucleus charge.

Introducing these values in Eqs. (2) and (6) we can obtain the differential cross section in the longitudinal recoil-ion momentum near $\lambda=0$,

$$\frac{d\sigma}{dp_{R||}}=2\pi v^2|f_c|^2\lambda\mathcal{G}(\lambda), \tag{8}$$

where $\mathcal{G}(\lambda)$ is determined from the series expansion (6) in λ. It is a regular function of λ as $\lambda\rightarrow 0$. The first few terms are given by

$$\mathcal{G}(\lambda)=4B_{00}+8B_{10}\lambda+O(\lambda^2). \tag{9}$$

As $\lambda\rightarrow 0$, two cases are of particular interest. If $Z_p>0$, we have

$$\frac{d\sigma}{dp_{R||}}\rightarrow 2\pi^2 Z_p v\mathcal{G}(\lambda). \tag{10}$$

Thus we have obtained that the longitudinal recoil-ion momentum distribution approaches a finite value in a way determined by the coefficients of the expansion Eq. (6) or Eq. (8). On the contrary, for negatively charged projectiles, as $\lambda\rightarrow 0$, we have

$$\frac{d\sigma}{dp_{R||}}\rightarrow 2\pi^2|Z_p|ve^{-\left[\frac{\pi|Z_p|}{\lambda v}\right]}\mathcal{G}(\lambda). \tag{11}$$

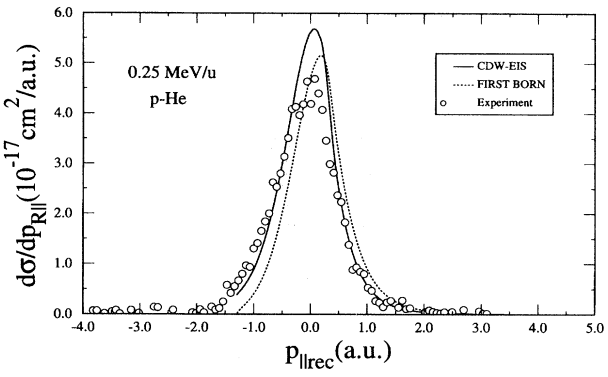

FIG. 2. The longitudinal recoil-ion momentum distribution for single ionization of He by protons at 250 keV/u. Experimental data are from Dörner *et al.* [1]. Solid line, present CDW-EIS calculation; dashed line, present first Born calculation.

The longitudinal momentum distribution approaches zero exponentially.

Therefore the longitudinal recoil-ion momentum distributions for ion-atom ionization by proton impact and by antiproton impact will have a very different behavior near the threshold. These differences between positively and negatively charged projectiles come from the differences in the DDCS. At $\vec{k}_e=\vec{v}$, the DDCS has a cusp for positively charged projectiles (e.g., protons) and an anticusp (or dip) for the negatively charged projectiles (e.g., antiprotons) [6]. Experiments on the longitudinal recoil-ion momentum distributions in the ionization of atoms by antiprotons should provide a good test to our predictions.

If the DDCS is evaluated using the first Born theory, $d\sigma/dp_{R||}$ would approach zero at the threshold for *both* positively and negatively charged projectiles. This is because the DDCS calculated from the first Born approximation does not have the singularity at $\vec{k}_e=\vec{v}$. And the integral in Eq. (2) goes to zero identically as $\lambda\rightarrow 0$. Thus the finite longitudinal recoil-ion momentum distribution at $p_{R||}^{min}$ is a direct reflection of the Coulomb interaction between the projectile and the ionized electron in the exit channel.

We are not aware of any previous work on the longitudinal recoil-ion momentum distribution at the threshold and its interpretation as due to ECC electrons. Our analysis is consistent with the recent experiment of Dörner *et al.*, where the longitudinal momentum distributions of He^+ ions are measured in the single ionization of the He atom by proton impact [1]. The measured longitudinal recoil-ion momentum distributions for ionization of He by protons at an impact energy of 250 keV/u are presented in Fig. 2. The kinematical threshold $p_{R||}^{min}$ is approximately at -1.296 a.u. The measured data below $p_{R||}^{min}$ could be ascribed to background noise and should be discarded. In the same figure, we have shown two theoretical calculations based on the *continuum-distorted-wave-eikonal-initial state* (CDW-EIS) method [7] (solid lines) and the first Born approximation (dashed lines). At intermediate and high energies, the CDW-EIS method has proven to be a successful method for studying the ionization process. Compared with other perturbative methods the

CDW-EIS method has the advantage that it uses wave functions with correct asymptotic Coulomb boundary conditions. We followed the independent electron model of Fainstein, Ponce, and Rivarola [6] to treat two-electron target atoms. The initial He ground state is described by the Hartree-Fock approximation, while the final state is given by the hydrogenic wave function with an effective charge.

The CDW-EIS calculations show rather good agreement with the experiment near the threshold, $p_{R||}^{min}$. The CDW-EIS theory also agrees well with the experiment in the *full* range of the longitudinal recoil-ion momentum. The broad peak is mainly due to the soft-electron emissions, which will be analyzed next. As expected, the first Born approximation is not sufficient to explain the behavior of longitudinal recoil-ion momentum distributions near the threshold. It approaches zero identically at $p_{R||}^{min}$.

Soft-electron emission. In Fig. 1, low-energy or soft electrons are distributed mostly around $p_{R||}=p_{R||}^{s}=|\varepsilon_i|/v$, at which point electrons can be emitted with *zero* energy at *all* angles. This region contributes most to the total ionization cross section. It gives rise to the so-called soft-collision (SC) peak in the single differential cross section, $d\sigma/d\varepsilon_e$. In general, the DDCS around the soft-electron peak can be parametrized as [8]

$$\frac{d^2\sigma}{d\varepsilon_e d(\cos\theta_e)}=[\beta_0(\varepsilon_e)+\beta_1(\varepsilon_e)P_1(\cos\theta_e)+\beta_2(\varepsilon_e)P_2(\cos\theta_e)], \tag{12}$$

where $P_l(\cos\theta_e)$ is the lth order Legendre polynomial.

We now consider the different consequences of the DDCS above on the longitudinal recoil-ion momentum distribution. If $\beta_1=0$, the DDCS for the soft electrons is isotropic and the maximum of $d\sigma/dp_{R||}$ would be given at $p_{R||}=p_{R||}^{s}=|\varepsilon_i|/v$. If $\beta_1>0$, the forward electrons are enhanced in the DDCS. In this case, the maximum of the momentum distribution $d\sigma/dp_{R||}$ is shifted towards a lower $p_{R||}$ according to Fig. 1. If $\beta_1<0$, the backward electrons are enhanced in the DDCS and the maximum for $d\sigma/dp_{R||}$ is shifted towards larger $p_{R||}$. In Fig. 2, the peak of the longitudinal momentum distribution is shifted from $p_{R||}^{s}\approx 0.286$ a.u. The measured peak position is at 0.07 a.u. The calculated peak position by the CDW-EIS theory is also at 0.07 a.u., in excellent agreement with the experiment. The first Born theory gives a peak position at 0.2 a.u. The measurements and calculations suggest that β_1 is positive for positively charged projectiles. This conclusion is in agreement with the findings of Suárez *et al.* [8] in their experimental study of DDCS spectra.

Note that for negatively charged projectiles, such as antiprotons, β_1 would be negative. Therefore, we predict that the soft-electron peak in the longitudinal momentum distribution would be shifted towards larger $p_{R||}$ from $p_{R||}^{s}$.

Binary electrons. Much attention has been given to the study of binary electrons (BE's) in the DDCS because of its pronounced peak structure. In the longitudinal recoil-ion momentum spectroscopy, we can identify binary electrons as those located at the $p_{R||}=0$ line, see Fig. 1. Along this line, for each given angle of θ_e, we generally have two electron momenta,

$$k_e^{\pm}=v\cos\theta_e\pm\sqrt{v^2\cos^2\theta_e-2|\varepsilon_i|}, \tag{13}$$

except at $\theta_e=\theta_e^{max}$, where $k_e^{-}=k_e^{+}=\sqrt{2|\varepsilon_i|}$. From this equation, it is clear that the binary electrons are emitted within the cone between $\theta_e=0$ and θ_e^{max}, where $\cos\theta_e^{max}=1/v\sqrt{2|\varepsilon_i|}$. At high collision energy, since $v^2/2\gg|\varepsilon_i|$, $k_e^{+}\approx 2v\cos\theta_e-|\varepsilon_i|/v\cos\theta_e$, which is close to the usual BE peak defined for scattering from a free electron. We note that there is another solution from Eq. (13), k_e^{-}. This energy would lie close to the soft-electron peak region and has been discussed by Fainstein, Ponce, and Rivarola [6]. In Fig. 2, the soft-electron peak should also include contributions from the soft BE's. We cannot easily identify these electrons unless other components of the momentum are measured.

We can now give a complete description of the longitudinal recoil-ion momentum distributions by combining the ECC, SC, and binary electrons with electrons located in other regions of Fig. 1. The line $p_{R||}=p_{R||}^{s}=|\varepsilon_i|/v$ divides $p_{R||}$ into two regions. For $p_{R||}<p_{R||}^{s}$, electrons can only be emitted in the forward directions. Low-energy (soft) electrons, high-energy ECC, and binary electrons are all included in this region. Electrons located in this region can be emitted within the cone defined by $0^\circ\leq\theta_e\leq\theta_{max}$, where

$$\cos(\theta_e^{max})=\frac{1}{v}\sqrt{2(|\varepsilon_i|-p_{R||}v)}. \tag{14}$$

For a given $p_{R||}$, the electron momentum k_e is a double valued function of θ_e, $k_e^{\pm}(p_{R||},\theta_e)$, as given in Eq. (2). As θ_e varies from 0° the two branches k_e^{+} and k_e^{-} eventually join at $\theta_e=\theta_e^{max}$. The locus of this joint point is given by the curve $k_e=k_e(\theta_e^{max},p_{R||})$ (see Fig. 1).

For $p_{R||}>p_{R||}^{s}$, $k_e(p_{R||},\theta_e)$ is a single valued function in θ_e. For $0^\circ\leq\theta_e\leq 90^\circ$, electrons are emitted in the forward direction. For $90^\circ\leq\theta_e\leq 180^\circ$, electrons are emitted in the backward direction. It is noted that in this region backward electrons are more important, as they have lower energies and are emitted in the opposite direction of the recoil ion. It is also possible to have more energetic electrons coming along the direction of the recoiling ion, but the longitudinal recoil-ion momentum distribution $d\sigma/dp_{R||}$ is expected to decrease rapidly with the increase of $p_{R||}$, since higher-energy electrons have smaller cross sections. This is consistent with the experimental measurement in Fig. 2.

In conclusion, we have analyzed the longitudinal recoil-ion momentum distribution in the single ionization process by considering the three-body kinematic relations. We are able to relate the finite value of the longitudinal recoil-ion momentum distribution at the kinematic threshold as an unambiguous proof of the divergence of the electron capture to the continuum cusp. We have expressed this finite value in terms of parameters that describe the ECC peak in the double differential cross section in electron energy and emission angle. We have also studied the soft-electron emission and

the binary electron collision. This study illustrates the complementary nature of experimental recoil-ion momentum spectroscopy and the conventional DDCS in ion-atom collisions.

We are grateful to R. Dörner and J. Ullrich for providing us experimental data. This work is supported by the Division of Chemical Sciences, Office of Basic Energy Sciences, Office of Energy Research, U.S. Department of Energy.

[1] R. Dörner, V. Mergel, L. Zaoyuan, J. Ullrich, L. Spielberger, R.E. Olson, and H. Schmidt-Böcking, J. Phys. B **28**, 435 (1995).

[2] R. Moshammer, J. Ullrich, M. Unverzagt, W. Schmidt, P. Jardin, R.E. Olson, R. Mann, R. Dörner, V. Mergel, U. Buck, and H. Schmidt-Böcking, Phys. Rev. Lett. **73**, 3371 (1994).

[3] G.B. Crooks and M.E. Rudd, Phys. Rev. Lett. **25**, 1599 (1970); K.G. Harrison and M. Lucas, Phys. Lett. **33A**, 149 (1970).

[4] M.W. Lucas and W. Steckelmacker, in *Proceedings of the Third Workshop on High-Energy Ion-Atom Collisions, Debrecen, Hungary 1987*, edited by D. Berenyi and G. Hock, Lecture Notes in Physics Vol. 294 (Springer-Verlag, Berlin, 1987), p. 229.

[5] R.O. Barrachina, J. Phys. B **23**, 2321 (1990).

[6] P.D. Fainstein, V.H. Ponce, and R.D. Rivarola, J. Phys. B **24**, 3091 (1991).

[7] D.S.F. Crothers and J.F. McCann, J. Phys. B **16**, 3239 (1983).

[8] S. Suárez, C. Garibotti, W. Meckbach, and G. Bernardi, Phys. Rev. Lett. **70**, 418 (1993).